Case study of inhomogeneous cloud parameter retrieval from MODIS data

Céline Cornet,[1] Jean-Claude Buriez,[1] Jérôme Riédi,[1] Harumi Isaka,[2] and Bernard Guillemet[2]

Received 22 February 2005; revised 31 March 2005; accepted 18 May 2005; published 6 July 2005.

[1] Cloud parameter retrieval of inhomogeneous and fractional clouds is performed for a stratocumulus scene observed by MODIS at a solar zenith angle near 60°. The method is based on the use of neural network technique with multispectral and multiscale information. It allows to retrieve six cloud parameters, i.e. pixel means and standard deviations of optical thickness and effective radius, fractional cloud cover, and cloud top temperature. Retrieved cloud optical thickness and effective radius are compared to those retrieved with a classical method based on the homogeneous cloud assumption. Subpixel fractional cloud cover and optical thickness inhomogeneity are compared with their estimates obtained from 250m pixel observations; this comparison shows a fairly good agreement. The cloud top temperature appears also retrieved quite suitably. **Citation:** Cornet, C., J.-C. Buriez, J. Riédi, H. Isaka, and B. Guillemet (2005), Case study of inhomogeneous cloud parameter retrieval from MODIS data, *Geophys. Res. Lett.*, *32*, L13807, doi:10.1029/2005GL022791.

1. Introduction

[2] Satellite observation is the only possible way to obtain the main properties of clouds and their variability at the global scale. Current satellite retrieval of cloud properties is based on the plane-parallel homogeneous cloud assumption [*Nakajima and Nakajima*, 1995]; two cloud parameters, usually optical thickness and effective radius, are retrieved from visible and near-infrared measurements. However, the validity of the homogeneous cloud assumption has been frequently questioned [*Loeb et al.*, 1997; *Buriez et al.*, 2001]. This simplifying assumption may induce significant errors in the retrieved cloud parameters. A part of the errors is related to the plane-parallel bias which is due to the subpixel variability and varies significantly with the pixel size [*Cahalan et al.*, 1994; *Davis et al.*, 1997; *Szczap et al.*, 2000]. Some studies [*Davis et al.*, 1997; *Marshak et al.*, 1998; *Oreopoulos et al.*, 2000] also showed that the cloud inhomogeneity tends to smooth as well as to rough the radiation fields. In the context of cloud parameter retrieval, such effects may lead to either overestimate or underestimate the cloud properties.

[3] Different attempts have been made to retrieve optical thickness or effective radius accounted for cloud inhomogeneity effects [*Marshak et al.*, 1998; *Oreopoulos et al.*, 2000; *Faure et al.*, 2002; *Iwabuchi and Hayasaka*, 2003] or to estimate errors in retrieved cloud optical thickness due to the homogeneous cloud assumption [*Varnai and Marshak*, 2001, 2002; *Iwabuchi and Hayasaka*, 2002]. Recently, *Faure et al.* [2001] and *Cornet et al.* [2004] have developed a method to retrieve cloud parameters characterizing fractional and inhomogeneous clouds. The method is based on the use of mapping neural network (MNN) to perform inversion of multispectral and multiscale observations provided by radiometers such as Global Imager (GLI) and Moderate Resolution Imaging Spectroradiometer (MODIS). In this paper, we adapt the method to MODIS data and present first results obtained from real measurements.

2. MODIS Data

[4] We selected a marine stratocumulus scene of 200 × 200 km^2 off the west coast of the USA (Figure 1). The satellite overpass time is 19H45 UTC on 9 February 2003. The solar zenith angle is around 60°, the viewing zenith angle varies from 15° to 35° and the relative azimuth angle is around 120° corresponding rather to the backward direction. We used the MODIS radiances in the bands 2, 6, 7 and 30 (0.865, 1.64, 2.13 and 11.03 μm) for the cloud parameter retrieval, while the band 19 (0.940 μm) is used to remove water vapor absorption from the bands 2, 6 and 7. This removal is done by using regression coefficients between the ratio $R_{0.865}/R_{0.940}$ and the water vapor transmission obtained from line-by-line calculations. The solar bands are corrected for the absorption due to O_3, CO_2, CH_4, and N_2O assuming a mid-latitude winter profile and using the MODIS cloud top pressure product [*Platnick et al.*, 2003]. For the thermal band, the atmospheric correction is not necessary if we replace the surface temperature by the observed clear-sky brightness temperature and the cloud top temperature by an equivalent cloud brightness temperature. In an operational algorithm, the right cloud top temperature can be calculated from this brightness temperature if the atmospheric profile above the cloud is known.

3. Retrieval of an Inhomogeneous and Fractional Cloud: MNN Method

3.1. Database Building

[5] We prepared the synthetic database for the neural network training as by *Cornet et al.* [2004]. The bounded cascade cloud model was used to generate different cloud fields of 128 × 128 elementary pixels of 50 × 50 m^2. The corresponding radiance fields (angular steps of 2.5° and 5° for zenithal and relative azimuthal angles) were computed with the Spherical Harmonics Discrete Ordinate Method [*Evans*, 1998]. We selected the same cloud scenes as by

[1] Laboratoire d'Optique Atmosphérique UMR CNRS 8518, Université des Sciences et Technologies de Lille, Villeneuve d'Ascq, France.
[2] Laboratoire de Météorologie Physique UMR CNRS 6016, Université Blaise Pascal, Aubière, France.

Copyright 2005 by the American Geophysical Union.
0094-8276/05/2005GL022791$05.00

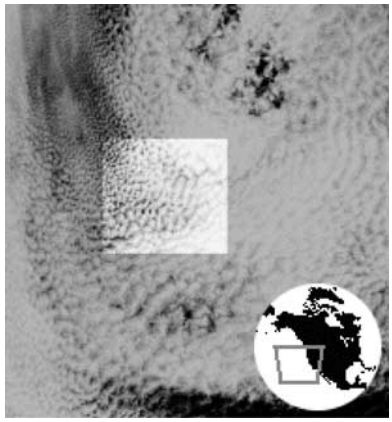

Figure 1. MODIS area used in this study. The MNN retrieval is applied to the highlighted part.

Cornet et al. [2004], but the cloud fields were assumed to be non-flat top clouds instead of flat top clouds. The cloud geometric depth was assumed to vary as the square root of the cloud optical thickness with a mean value of 300 m [*Minnis et al.*, 1992]. For the solar wavelengths, radiative transfer was simulated for the clouds with a fixed cloud base height of 1.20 km; the sea surface directional reflectance was computed for a wind speed of 5 $m.s^{-1}$and the aerosol contribution was simulated following *Smirnov et al.* [2002]. For the thermal band, radiative transfer simulations were done for three different cloud base heights (0.90, 1.20 and 1.50 km) and for three different surface temperatures (276, 280 and 284 K).

[6] The inverse cloud model is defined at 1 km scale (20×20 elementary pixels) with six cloud parameters: the fractional cloud cover *f*, the mean optical thickness on the pixel τ, the mean effective radius over cloudy part within a pixel Re, the standard deviation of optical thickness σ_τ, the standard deviation of effective radius σ_{Re} and the mean cloud top temperature T_c. The two inhomogeneity parameters (σ_τ, σ_{Re}) are useful to characterize and parameterize inhomogeneous clouds radiative effects [*Cahalan et al.*, 1994; *Szczap et al.*, 2000; *Lafont and Guillemet*, 2004].

[7] To retrieve these parameters, we define an input vector with nine components: the four area-averaged radiances ($R_{0.865}$, $R_{1.64}$, $R_{2.13}$ and $R_{10.8}$), the standard deviation of $R_{0.865}$ estimated over 1×1 km^2 pixels from 0.25×0.25 km^2 pixel radiance, the equivalent clear-sky surface temperature and three angular distances between a viewing geometry and the corresponding neural network one.

[8] The input vector has fewer components than the one used by *Cornet et al.* [2004]. Firstly, standard deviations for $R_{1.64}$ and $R_{2.13}$ are not available for MODIS; we tested that adding standard deviations estimated from 0.5×0.5 km^2 pixel radiance as input component did not improve the dispersion of retrieved cloud parameters. Secondly, we did not use the 3.75 μm radiance, since $R_{3.75}$ and $R_{2.13}$ contain redundant information and the correction of the thermal contribution in $R_{3.75}$ may also introduce some additional errors. However these tests were done only for a solar incidence at 60°; these conclusions could thus be different for other solar incidences, given the fact that thermal correction is more accurate for higher solar elevations [*Cornet et al.*, 2004].

3.2. Tests of the MNN Retrieval

[9] Before applying our retrieval procedure to real measurements, we tested it under different conditions. The first test is relative to the use of neural network for the cloud parameter retrieval. For this purpose, we trained especially MNNs to retrieve optical thickness and effective radius under the homogeneous cloud assumption from ($R_{0.865}$, $R_{2.13}$) radiance pairs. MNN retrieved values were compared with those of MODIS products [*Platnick et al.*, 2003]. The correlation between them are good with correlation coefficients of 0.999 for τ and 0.965 for Re respectively. However, the regression slopes are not exactly equal to unity, but close to 1.05 for τ and 1.10 for Re. These differences are probably due to some differences in radiative transfer modeling; in particular we assume a sea-surface directional reflectance instead of Lambertian one used for MODIS products. When a slight corrective factor to the MODIS products is applied to remove these biases, we obtain root mean square deviations (RMS) between modified MODIS and MNN, less than 5% of their corresponding means.

[10] For the second test, we retrieved the cloud parameters of a non-flat-top Gaussian cloud by using the MNNs trained with the non-flat-top bounded cascade clouds. The Gaussian process generates a synthetic cloud smoother than the bounded cascade leading to a cloud top variability less important. This two very different clouds allow us to test that neural networks are not too dependent on the cloud model used for their training. Table 1 shows that RMSEs and biases for each cloud parameter excepted for σ_{Re} are quite similar for both the types of clouds, which implies that the MNN retrieval is not too dependent on the cloud model assumption and therefore applicable to real data.

4. Inhomogeneous Cloud Parameters Retrieved From MODIS Data

[11] Our inhomogeneous cloud parameter retrieval algorithm was applied to the scene presented above; the "3D" denotes the cloud parameters retrieved with this method. The mean optical thickness τ_{3D} and mean effective radius Re_{3D} are compared to the modified MODIS products (part 3.2) τ_{1D} and Re_{1D} (Figure 2 and Table 2). Figure 2a shows that τ_{1D} is larger than τ_{3D} for most of the pixels, which implies a phenomenon of 'overbrightness', i.e. radiance larger than the plane-parallel one for a given optical thickness. This feature agrees with previous results showing that, when 1D theory is used, optical thickness is predom-

Table 1. RMSE Errors and Biases Obtained Between Retrieved and Initial Cloud Parameters for Two Types of Cloud Model: the Bounded Cascade Cloud and the Gaussian Cloud Models (θ_0 = 57.5° and 58°; θ_v = 15°; φ_v = 125°)

	τ	Re, μm	σ_τ	σ_{Re}, μm	*f*	T_c, K
			Bounded Cascade Cloud			
Range	0–41	0–28	0–22	0–13	0–1	267–279
RMSE	1.81	1.23	1.41	1.15	0.07	0.52
Bias	0.00	0.18	0.02	0.00	0.00	−0.01
			Gaussian Cloud			
Range	2–15	1–9	1–7	0–5	0.2–1	276–277
RMSE	0.80	1.04	0.95	1.74	0.08	0.41
Bias	0.47	−0.74	−0.32	−1.11	−0.04	0.12

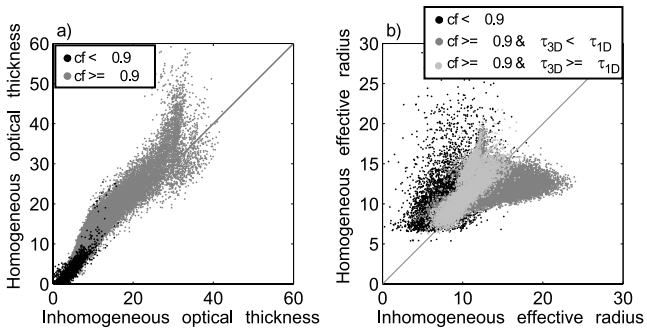

Figure 2. Comparison of cloud parameter retrieval at 1 km with the inhomogeneous cloud model (MNN method) and with the homogeneous cloud model (MODIS product). (a) Optical thickness; (b) effective radius.

inantly overestimated for oblique solar incidence [*Varnai and Marshak*, 2002; *Iwabuchi and Hayasaka*, 2002]. Moreover, the difference between τ_{3D} and τ_{1D} seems to increase with the optical thickness, which is consistent with illuminating effects that are higher for brighter radiances [*Loeb et al.*, 1997; *Varnai and Marshak*, 2001]. On the contrary, in the case of fractional cloud cover ($f < 0.9$), τ_{1D} is slightly smaller than τ_{3D} (bias ~ -1.05) possibly because of shadowing effects and/or plane-parallel bias.

[12] For effective radius (Figure 2b), the results are presented by separating them into three groups: the first group is composed of pixels with $f < 0.9$; the two other groups corresponding to $f \geq 0.9$ are separated following the sign of $\tau_{1D}-\tau_{3D}$. If we assume that optical thickness and effective radius are affected in the same manner by shadowing and illuminating effects, we can use this difference to characterize the difference between MNN and MODIS effective radius.

[13] According to *Platnick et al.* [2003], Re_{1D} appears often larger than Re_{3D} for fractional cloud cases. Figure 2b shows that for $f < 0.9$ the retrieved Re_{1D} is effectively larger than Re_{3D} and exhibits larger dispersion; it seems thus that MNN method deals better subpixel fractional cloud cover. For the second group ($\tau_{3D} \geq \tau_{1D}$), which should correspond to shadowing effect or plane-parallel bias, Re_{1D} is effectively larger than Re_{3D} for almost pixels. Since shadowing effects or plane-parallel bias relative to optical thickness make near infrared radiances apparently smaller, Re_{1D} appears larger than Re_{3D} as if there were larger absorption [*Szczap et al.*, 2000]. For the third group ($\tau_{3D} < \tau_{1D}$) corresponding rather to illuminating area, Re_{1D} is smaller than Re_{3D} for most of the pixels. This behavior can be explained by illuminating effects which make near-infrared radiances brighter.

[14] We analyzed the correlation between τ_{3D} and Re_{3D} (not shown). The correlation is positive for $\tau_{3D} < 15$ and negative for $\tau_{3D} > 15$. This behavior agrees with earlier observations [*Nakajima and Nakajima*, 1995]. *Lohmann et al.* [2000] also suggested that such change of sign in τ-Re correlation can correspond to the transition from non-precipitating to precipitating clouds. These two types of correlations also correspond to two different types of cloud appearance in Figure 1, i.e. the area with fractional cloud cover and the upper and lower right corners where clouds appear more compact and developed. However, it has to be considered carefully because for the group $\tau_{3D} > 15$, some MODIS input components, in particular the standard deviation of visible radiances, are slightly outside of the data range covered by the training database.

Table 2. Root Mean Square Differences and Biases (1D Minus 3D Retrieval)[a]

	RMSE (τ)	$\bar{\tau}_{1D} - \bar{\tau}_{3D}$	RMSE (re)	$\overline{re}_{1D} - \overline{re}_{3D}$
All	3.49 (28%)	+1.66	3.27 (28%)	−0.43
$F < 0.9$	1.42 (54%)	−1.05	4.14 (38%)	+2.78
$F \geq 0.9$	3.73 (27%)	+2.13	3.09 (25%)	−0.98
& $\tau_{3D} < \tau_{1D}$			3.43 (28%)	−1.66
& $\tau_{3D} \geq \tau_{1D}$			1.76 (16%)	+1.01

[a]The relative RMS differences are reported in parentheses. The results are separated following the different groups of Figure 2.

[15] With regard to the optical thickness inhomogeneity σ_τ and fractional cloud cover f, we compared our results with two equivalent parameters computed from the 250 m-visible radiance field. For σ_τ, we compared the relative standard deviation σ_τ/τ_{3D} to the relative standard deviation of radiances. To estimate an equivalent fractional cloud cover, we used a threshold, $[R_{min} + (R_{max} - R_{min})/5]$, derived from extreme reflectance values of the scene, to classify pixels as cloudy or clear. These estimations are relevant only if we have enough pixels to compute it. Accordingly, we retrieved these cloud parameters at 4 km scale. The input vector components are the $(4\ km)^2$ averaged radiances and the standard deviation of $R_{0.865}$ estimated from 1 km^2 pixels. Figure 3 shows that the two correlation coefficients are high and the RMS difference for f is only 0.06. These two parameters appear thus well retrieved at 4 km scale and we can expect that it is also correct at 1 km scale.

[16] Figure 4 presents two probability distributions of the cloud top temperature. The first distribution obtained under the homogeneous assumption exhibits two marked modes at 273.5K and 277K. The homogeneous retrieval is based on the assumption of opaque cloud. However, for fractional cloud cover or thin cloud, there is a positive bias due to the surface temperature (here, $\overline{T_s} = 286K$) [*Platnick et al.*, 2003]. For inhomogeneous clouds with fractional cloud cover, cloud top height should not vary from one cloud to the others and the equivalent cloud top temperature appears more uniform over the cloud scene. The temperature for inhomogeneous clouds is slightly lower than the MODIS one because, for this case study, we did not remove the atmospheric constituent effects whereas it is done for the MODIS temperature.

[17] We do not have any way to verify the consistency of the effective radius inhomogeneity. We analyzed the corre-

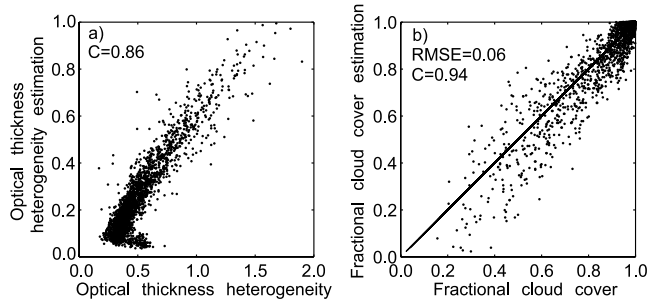

Figure 3. (a) σ_τ and (b) f retrieved at 4 km scale compared to an estimation of these two parameters calculated from the 250 m-visible radiances.

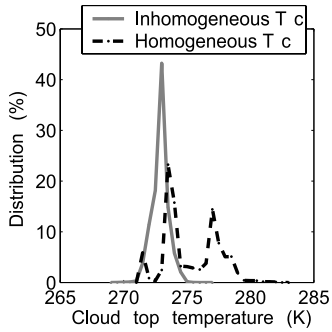

Figure 4. Comparison of cloud top temperature distribution.

lation between Re_{3D} and σ_{Re}, which shows that σ_{Re} increases with Re_{3D}, but exhibits a rather large dispersion. However, we have to consider cautiously the retrieval of this parameter, because the present input vector does not include the standard deviation of 2.15 μm radiance; consequently it is provided only with little information on this parameter.

5. Discussions and Perspectives

[18] The aim of this paper is to apply to real data a method of neural network cloud parameter retrieval previously developed for fractional and inhomogeneous cloud [*Faure et al.*, 2001; *Cornet et al.*, 2004]. The retrieval algorithm was adapted to MODIS data for this case study and the results were presented for 6 cloud parameters.

[19] We compared retrieved optical thickness and effective radius with MODIS products. The deviations between the two agree with previous studies about differences between inhomogeneous and homogeneous cloud effects. Retrieved fractional cloud cover and optical thickness heterogeneity are quite consistent with an estimation of this two parameters and cloud top temperature appears less biased by the surface temperature than the MODIS cloud top temperature.

[20] Looking at the liquid water path of this scene that can be easily derived from τ and Re, we obtain 97 g.m^{-2} from MODIS retrieval and 85 g.m^{-2} from MNN retrieval, which corresponds to a difference of about 15% for this scene.

[21] Even if some of the results have to be considered carefully, retrievals obtained with the MNN method appear quite satisfactory and significantly different from those obtained under the homogeneous assumption. In order to apply this retrieval more generally on MODIS data, we have to be very careful during the database building. The training set used has to cover with a sufficient sampling all the possible range of real data, that implies several difficulties already discussed by *Cornet et al.* [2004]. For example, still more tests should be done to be quite sure that the results are not biased by the cloud model used for the training. Further improvements can also be planned, in particular by using the neighboring pixel information [*Faure et al.*, 2002; *Iwabuchi and Hayasaka*, 2003] and by estimating output neural network uncertainties [*Aires et al.*, 2004].

[22] **Acknowledgments.** MODIS data were obtained from NASA Goddard Earth Sciences DAAC. Support received from Région Nord-Pas de Calais is gratefully acknowledged.

References

Aires, F., C. Pringent, and W. B. Rossow (2004), Neural network uncertainty assessment using Bayesian statistics with application to remote sensing: 2 Output errors, *J. Geophys. Res.*, *109*, D10304, doi:10.1029/2003JD004174.

Buriez, J. C., M. Doutriaux-Boucher, F. Parol, and N. G. Loeb (2001), Angular variability of the liquid water cloud optical thickness retrieved from ADEOS-POLDER, *J. Atmos. Sci.*, *58*, 3007–3018.

Cahalan, R. F., W. Ridgway, W. J. Wiscombe, and T. L. Bell (1994), The albedo of fractal stratocumulus clouds, *J. Atmos. Sci.*, *51*, 2434–2455.

Cornet, C., H. Isaka, B. Guillemet, and F. Szczap (2004), Neural network retrieval of cloud parameters of inhomogeneous clouds from multispectral and multiscale radiance data: Feasibility study, *J. Geophys. Res.*, *109*, D12203, doi:10.1029/2003JD004186.

Davis, A., A. Marshak, R. F. Cahalan, and W. Wiscombe (1997), The Landsat scale break in stratocumulus as a three-dimensional effect: Implications for cloud remote sensing, *J. Atmos. Sci.*, *54*, 241–260.

Evans, K. F. (1998), The spherical harmonics discrete ordinate method for three-dimensional atmospheric radiative transfer, *J. Atmos. Sci.*, *55*, 429–446.

Faure, T., H. Isaka, and B. Guillemet (2001), Neural network retrieval of cloud parameters of inhomogeneous and fractional clouds: Feasibility study, *Remote Sens. Environ.*, *77*, 123–138.

Faure, T., H. Isaka, and B. Guillemet (2002), Neural network retrieval of cloud parameters from high-resolution multi-spectral radiometric data: A feasibility study, *Remote Sens. Environ.*, *80*, 285–296.

Iwabuchi, H., and T. Hayasaka (2002), Effects of cloud horizontal inhomogeneity on the optical thickness retrieved from moderate-resolution satellite data, *J. Atmos. Sci.*, *59*, 2227–2242.

Iwabuchi, H., and T. Hayasaka (2003), A multi-spectral non-local method for retrieval of boundary layer cloud properties from optical remote sensing data, *Remote Sens. Environ.*, *88*, 294–308.

Lafont, D., and B. Guillemet (2004), Subpixel fractional cloud cover and inhomogeneity effects on microwave beam-filling error, *Atmos. Res.*, *72*, 149–168.

Loeb, N. G., T. Varnai, and R. Davies (1997), Effects of cloud inhomogeneities on the solar zenith angle dependence of nadir reflectance, *J. Geophys. Res.*, *102*, 9395–9397.

Lohmann, U., G. Tselioudis, and C. Tyler (2000), Why is the cloud albedo–particle size relationship different in optically thick and optically thin clouds?, *Geophy. Res. Lett.*, *27*, 1099–1102.

Marshak, A., A. Davis, R. F. Cahalan, and W. Wiscombe (1998), Non local independent pixel approximation: Direct and inverse problems, *IEEE Trans. Geosci. Remote Sens.*, *36*, 192–205.

Minnis, P., P. W. Heck, D. F. Young, C. W. Fairall, and J. B. Snider (1992), Stratocumulus cloud properties derived from simultaneous satellite and island-based instrumention during FIRE, *J. Appl. Meteorol.*, *31*, 317–339.

Nakajima, T. Y., and T. Nakajima (1995), Wide-area determination of cloud microphysical properties from NOAA AVHRR measurements for FIRE and ASTEX regions, *J. Atmos. Sci.*, *52*, 4043–4059.

Oreopoulos, L., R. F. Cahalan, A. Marshak, and G. Wen (2000), A new normalized difference cloud retrieval technique applied to Landsat radiances over the Oklahoma ARM site, *J. Appl. Meteorol.*, *39*, 2305–2321.

Platnick, S., M. D. King, S. A. Ackerman, W. P. Menzel, B. A. Baum, J. C. Riédi, and R. A. Frey (2003), The MODIS cloud products: Algorithms and examples from Terra, *IEEE Trans. Geosci. Remote Sens.*, *41*, 459–473.

Smirnov, A., B. N. Holben, Y. J. Kaufman, O. Dubovik, T. F. Eck, I. Slutsker, C. Pietras, and R. N. Halthore (2002), Optical properties of atmospheric aerosol in maritime environments, *J. Atmos. Sci.*, *59*, 501–523.

Szczap, F., H. Isaka, M. Saute, B. Guillemet, and A. Ioltukhovski (2000), Effective radiative properties of bounded cascade absorbing clouds: Definition of effective single scattering albedo, *J. Geophys. Res.*, *105*, 20,635–20,648.

Varnai, T., and A. Marshak (2001), Statistical analysis of the uncertainties in cloud optical depth retrievals caused by three-dimensional radiative effects, *J. Atmos. Sci.*, *58*, 1540–1548.

Varnai, T., and A. Marshak (2002), Observations of three-dimensional radiative effects that influence MODIS cloud optical thickness retrievals, *J. Atmos. Sci.*, *59*, 1607–1618.

J.-C. Buriez, C. Cornet, and J. Riédi, Laboratoire d'Optique Atmosphérique UMR CNRS 8518, Université des Sciences et Technologies de Lille, Villeneuve d'Ascq, F-59655 France. (celine.cornet@loa.univ-lille1.fr)

B. Guillemet and H. Isaka, Laboratoire de Météorologie Physique UMR CNRS 6016, Université Blaise Pascal, F-63177 Aubière, France.